

Layered Materials

SPECIAL  
ISSUE

# Intercalation Pseudocapacitance of Exfoliated Molybdenum Disulfide for Ultrafast Energy Storage

Hyun Deog Yoo,<sup>[a]</sup> Yifei Li,<sup>[a]</sup> Yanliang Liang,<sup>[a]</sup> Yucheng Lan,<sup>[b]</sup> Feng Wang,<sup>[c]</sup> and Yan Yao<sup>\*[a, d]</sup>

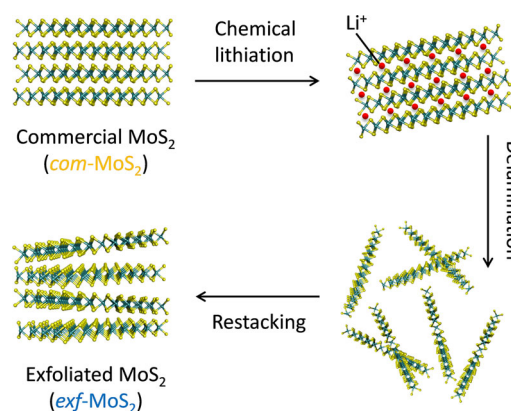
**Abstract:** We report intercalation pseudocapacitance of 250 F g<sup>-1</sup> for exfoliated molybdenum disulfide (MoS<sub>2</sub>) in non-aqueous electrolytes that contain lithium ions. The exfoliated MoS<sub>2</sub> shows surface-limited reaction kinetics with high rate capability up to 3 min of charge or discharge. The intercalation pseudocapacitance originates from the extremely fast kinetics due to the enhanced ionic and electronic transport enabled by the slightly expanded layer structure as well as the metallic 1T-phase. The exfoliated MoS<sub>2</sub> could be also used in a Li-Mg-ion hybrid capacitor, which shows full cell specific capacitance of 240 F g<sup>-1</sup>.

Li ions intercalate and diffuse inside the interlayer gap of layered materials such as graphite, lithium cobalt oxide, and molybdenum disulfide (MoS<sub>2</sub>).<sup>[1–3]</sup> Recently, intercalation pseudocapacitance has drawn much attention because of the significantly larger capacitance compared to conventional supercapacitors while maintaining the high-rate capability as a supercapacitor.<sup>[4–7]</sup> Intercalation pseudocapacitance, which occurs when ions intercalate into the tunnels or layers of a redox-active material accompanied by a faradaic charge-transfer with no crystallographic phase change, is one of three mechanisms that give rise to pseudocapacitance.<sup>[6]</sup> Mesoporous and nanocrystalline oxides were found to exhibit pseudocapacitive be-

haviors through rapid ion intercalation.<sup>[4,5]</sup> Recently, M. Chhwalla et al. reported that layered molybdenum sulfides also displayed intercalation pseudocapacitance when exfoliated into nanosheets and then restacked.<sup>[7]</sup> However, the capacity was limited to 100 F g<sup>-1</sup> in aqueous electrolyte and less than 60 F g<sup>-1</sup> in organic electrolyte.

In this work, we improved the capacitance of exfoliated-restacked MoS<sub>2</sub> to 250 F g<sup>-1</sup> in an organic Li-ion-containing electrolyte. Electrochemical characterization confirmed the ultrafast kinetics mechanism as surface-limited intercalation pseudocapacitance. We also demonstrated a Li-Mg-ion hybrid capacitor with full-cell capacitance of about 240 F g<sup>-1</sup>, six times higher than that of conventional activated carbon-based supercapacitors.

We synthesized exfoliated and restacked molybdenum disulfide (*exf*-MoS<sub>2</sub>) according to Scheme 1. The crystallinity of *exf*-MoS<sub>2</sub> was substantially reduced compared to that of *com*-MoS<sub>2</sub> (Figure 1a). The (002) peak of *com*-MoS<sub>2</sub> corresponds to an interlayer distance of 0.61 nm. For the *exf*-MoS<sub>2</sub> sample we ob-



**Scheme 1.** Exfoliation of MoS<sub>2</sub> through a chemical lithiation, delamination, and restacking approach.

served a weaker and broader (001) peak corresponding to an increased interlayer distance of 0.64 nm. Note that the (001) peak of *exf*-MoS<sub>2</sub> corresponds to the (002) peak of *com*-MoS<sub>2</sub> because of the *P6<sub>3</sub>/mmc* and *P1* symmetry of 2H and 1T phase, respectively.<sup>[8]</sup> Both peaks essentially correspond to the same interlayer spacing between MoS<sub>2</sub> slabs. Metallic 1T-phase of *exf*-MoS<sub>2</sub> was clearly evidenced due to the appearance of hexagonal patterns of  $a\sqrt{3} \times a\sqrt{3}$  superstructure inside the (100) electron diffraction (ED) ring (Figure 1b).<sup>[9,10]</sup> The amorphous

[a] Dr. H. D. Yoo, Y. Li, Dr. Y. Liang, Prof. Y. Yao  
Department of Electrical & Computer Engineering and  
Materials Science and Engineering Program  
University of Houston  
Houston, TX 77204 (USA)  
E-mail: yyao4@uh.edu

[b] Dr. Y. Lan  
Department of Physics and Engineering Physics  
Morgan State University  
Baltimore, MD 21251 (USA)

[c] Dr. F. Wang  
Sustainable Energy Technologies Department  
Brookhaven National Laboratory  
Upton, NY 11973 (USA)

[d] Prof. Y. Yao  
Texas Centre for Superconductivity  
University of Houston  
Houston, TX 77204 (USA)

This manuscript is part of a Special Issue on Nanomaterials for Energy Conversion and Storage. A link to the Table of Contents will appear here once the Special Issue is assembled.

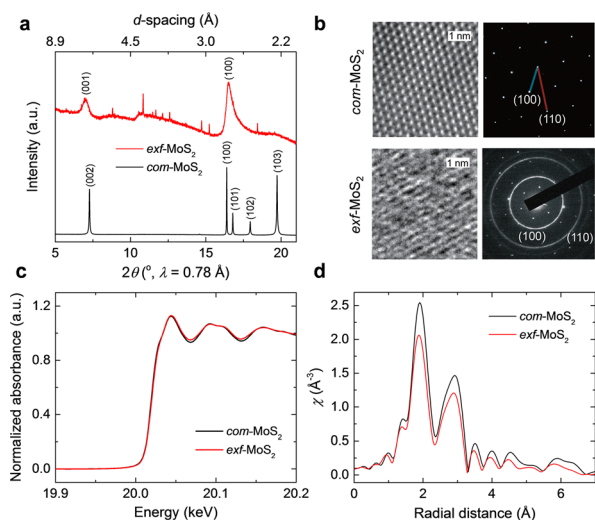


**Figure 1.** Material characterization of commercial (*com-*) and exfoliated (*exf-*) MoS<sub>2</sub>: (a) XRD patterns, (b) TEM images and the electron diffraction patterns, (c) XANES and (d) EXAFS spectra for molybdenum K edge.

structure is reflected in the ring-shaped ED pattern. Although the interlayer distance slightly expanded, the oxidation state and bond length kept intact. No shift of the Mo K edge was observed for the two samples from the X-ray absorption near edge structure (XANES, Figure 1c). The extended X-ray absorption fine structure data (EXAFS, Figure 1d) shows the same bond length for Mo-S (1.9 Å) and Mo-Mo (2.9 Å) before and after exfoliation.<sup>[11]</sup> Metallic 1T-phase and semiconducting 2H-phase coexist in *exf-MoS<sub>2</sub>* with the ratio of 2:3 obtained from the X-ray photoelectron spectroscopy as reported in our previous work.<sup>[12]</sup> The 40% 1T phase is above the percolation threshold to form an electronic conductive pathway to significantly enhance the electronic conductivity compared to that of *com-MoS<sub>2</sub>*.<sup>[13,14]</sup> It is well known that *com-MoS<sub>2</sub>* also undergoes phase transition from 2H to 1T during the first discharge step.<sup>[8,10,15]</sup> Therefore, both *exf-MoS<sub>2</sub>* and cycled *com-MoS<sub>2</sub>* have similar 1T-phase with the major difference coming from the slightly expanded interlayer distance and the lower crystallinity of *exf-MoS<sub>2</sub>*.

In the cyclic voltammogram, current (*i*) was normalized by scan rate (*v*) to present the normalized current (*i v*<sup>-1</sup>), which is equivalent to capacitance in Fg<sup>-1</sup>. The normalized current of *com-MoS<sub>2</sub>* reduces significantly as the scan rate increases (Figure 2a), and the peak current is proportional to the square root of scan rate (Figure 2b). This behavior reveals that the intercalation of Li<sup>+</sup> into *com-MoS<sub>2</sub>* is solid-state diffusion limited.<sup>[16]</sup> On the other hand, *exf-MoS<sub>2</sub>* shows nearly constant normalized current with respect to the scan rate (Figure 2c). The fact that peak current is linearly proportional to the scan rate (Figure 2d) shows the reaction kinetics becomes surface limited.<sup>[5,16]</sup> As a result, structural change from *com-MoS<sub>2</sub>* to *exf-MoS<sub>2</sub>* resulted in the shift of kinetic behavior from diffusion-limited in *com-MoS<sub>2</sub>* to surface-limited in *exf-MoS<sub>2</sub>*, therefore exhibiting high rate capability.<sup>[6]</sup>

The rapid intercalation of Li<sup>+</sup> is correlated with the slightly expanded layer structure that lowers the migration barrier of

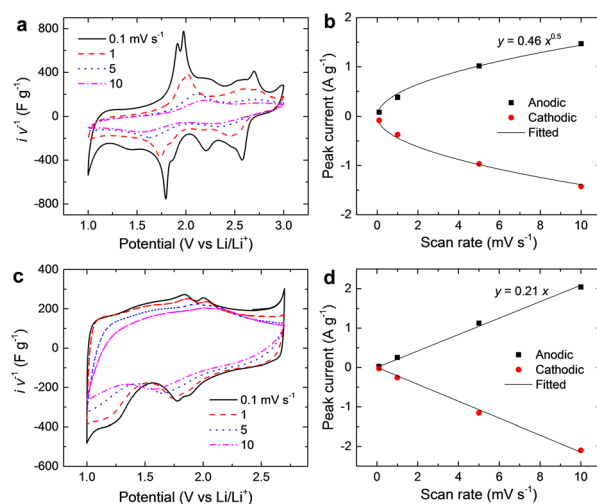


**Figure 2.** Mechanistic study of Li-ion intercalation into MoS<sub>2</sub>: cyclic voltammograms of *com-MoS<sub>2</sub>* (a) and *exf-MoS<sub>2</sub>* (c); peak current vs. scan rate and fitting for *com-MoS<sub>2</sub>* (b) and *exf-MoS<sub>2</sub>* (d).

solid-state Li<sup>+</sup> diffusion in between the MoS<sub>2</sub> layers,<sup>[17]</sup> as well as the high electronic conductivity of the metallic 1T-phase. According to the Nernst equation, the intercalation pseudocapacitance (*C<sub>p</sub>*, Fg<sup>-1</sup>) is given by a function of occupancy fraction of layer lattice sites (*x*) as in Equation (1):

$$C_p(x) = Q_0 \frac{dx}{dE} = \frac{Q_0 F}{RT} x(1-x) \quad (1)$$

where, *Q<sub>0</sub>*, *E*, *F*, *R*, and, *T* denote the specific capacity (Cg<sup>-1</sup>), electrode potential (V), Faraday constant (Cmol<sup>-1</sup>), Gas constant (Jmol<sup>-1</sup>K<sup>-1</sup>), and temperature (K), respectively. According to Eq. (1), the pseudocapacitance is represented by the peak-shaped voltammogram that is maximized at *x*=0.5.<sup>[18]</sup> In, *exf-MoS<sub>2</sub>*, however, the intercalation pseudocapacitance shows a quite flat voltammogram (Figure 2c). This flat voltammogram is attributed to the variation of site energy caused by the structural disorder.<sup>[19]</sup> Flat voltammograms have often been observed from other pseudocapacitive materials such as ruthenium oxide where multiple redox couples are involved.<sup>[20]</sup> Note that the surface area of *exf-MoS<sub>2</sub>* is surprisingly less than that of *com-MoS<sub>2</sub>* (4.3 vs. 9.4 m<sup>2</sup>g<sup>-1</sup>), probably due to the formation of larger flakes during the restacking process.<sup>[12]</sup> The contribution of the electric double-layer capacitance was therefore estimated to be at most 2% of the total capacitance of *exf-MoS<sub>2</sub>*, assuming the usual double-layer capacitance value of 10–50 μFcm<sup>-2</sup>.

The intercalation pseudocapacitance of *exf-MoS<sub>2</sub>* was further confirmed by electrochemical impedance spectroscopy (EIS). EIS was measured at varied electrode potentials from 2.5 V to 1.0 V vs. Li/Li<sup>+</sup>. The Nyquist plot shows significant decrease in the charge transfer resistance as the potential is lowered to 1.0 V vs. Li/Li<sup>+</sup> (Figure 3a). This phenomena agrees with the prediction from the Butler–Volmer kinetics where the charge transfer resistance decreases at large overpotential.<sup>[21]</sup> Note the real part of the capacitance (*C'*) represents the capacitance

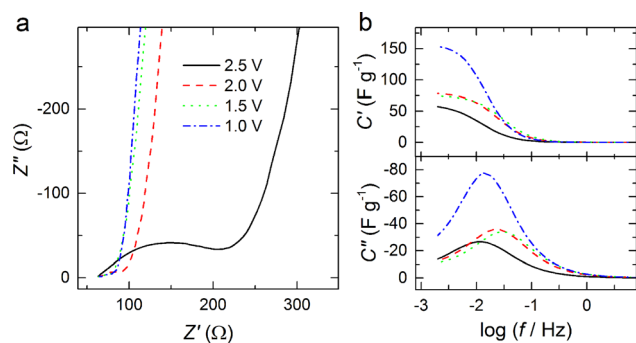


**Figure 3.** EIS results demonstrate the capacitive behaviors of *exf*-MoS<sub>2</sub> at various potentials (vs. Li/Li<sup>+</sup>): (a) the Nyquist plot and (b) complex capacitance plot vs. frequency.

value of the electrode at a given potential,<sup>[22]</sup> which increases from 50 to 150 Fg<sup>-1</sup> from 2.5 to 1.0 V vs. Li/Li<sup>+</sup> (Figure 3b, top). The characteristic frequency defined as the peak frequency in the C'' vs. log f plot (Figure 3b, bottom) is about 13 mHz, which corresponds to a response time of about 1.3 min.

Both *com*-MoS<sub>2</sub> and *exf*-MoS<sub>2</sub> show the same specific capacity of 140 mAh g<sup>-1</sup> at 0.1C rate (Figure 4a), which is close to the

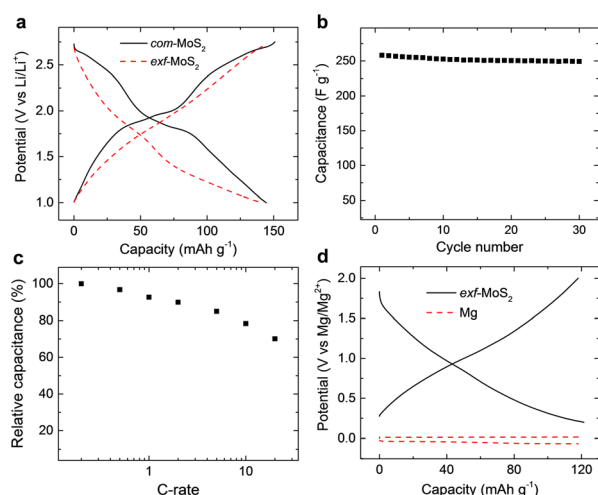


**Figure 4.** Li-ion intercalation pseudocapacitance: (a) voltage profile at 0.1C, (b) capacitance retention at 1C rate, (c) rate performance, (d) voltage profile of a Li-Mg hybrid capacitor with the potential of both electrodes measured simultaneously.

theoretical capacity of LiMoS<sub>2</sub> (167 mAh g<sup>-1</sup>). The fact we observed the same capacity for both samples supports that the number of intercalation sites does not change during the preparation of *exf*-MoS<sub>2</sub>. The lower voltage profile for *exf*-MoS<sub>2</sub> is related to the broad distribution of site energy due to the disordered structure compared to the crystalline, *com*-MoS<sub>2</sub>.<sup>[19]</sup> Capacitance of about 250 Fg<sup>-1</sup> is preserved with the cycling of *exf*-MoS<sub>2</sub> at 1C rate for 30 cycles (Figure 4b), which is calculated using  $C = 3.6Q/V$ , where Q is 140 mAh g<sup>-1</sup> and V is 2 V. It is noteworthy that the capacitance is far larger than the maximum capacitance of the state-of-the-art electric double-layer

capacitors (EDLCs), which shows about 100–150 Fg<sup>-1</sup> in non-aqueous electrolytes.<sup>[23]</sup> The rapid intercalation enabled the high capacitance of 150 Fg<sup>-1</sup> (i.e., utilization of 70%) even at 20C, which is equivalent to 3 min charge or discharge (Figure 4c). M. Chhowalla recently demonstrated ≈60 Fg<sup>-1</sup> intercalation pseudocapacitance in organic electrolyte using *exf*-MoS<sub>2</sub> prepared in a similar method.<sup>[7]</sup> The fact that we obtained 300% higher capacity may be due to the smaller size of Li<sup>+</sup> than EMIM<sup>+</sup> cations used in their study, therefore allowing a larger amount of Li<sup>+</sup> to be intercalated.

The intercalation pseudocapacitor electrode can also be applied in various configurations.<sup>[24]</sup> We demonstrate a hybrid Mg-Li supercapacitor in Figure 4d that can maximize the utilization of large intercalation pseudocapacitance by pairing *exf*-MoS<sub>2</sub> with a magnesium metal anode.<sup>[25]</sup> Magnesium anode shows a flat deposition/dissolution voltage profile (slope ≈0) with high gravimetric (2205 mAhg<sup>-1</sup>) and volumetric capacity (3833 mAhcc<sup>-1</sup>). So the capacitance, which is inversely proportional to the slope of the voltage profile, is virtually infinite (∞). Moreover, the magnesium metal anode is not susceptible to dendrite growth, in contrast to dendritic deposition of Li metal anode. Moreover, Mg metal shows excellent rate capability that could match with supercapacitor cathodes.<sup>[25]</sup> The Mg hybrid intercalation pseudocapacitor attained full-cell capacitance of about 240 Fg<sup>-1</sup> at 0.1C rate, considering the total mass of both *exf*-MoS<sub>2</sub> and Mg metal electrodes (Figure 4d). The full-cell capacitance is 6 times higher than that of symmetric supercapacitors based on activated carbon electrodes, which is usually 30–40 Fg<sup>-1</sup>.<sup>[26]</sup>

In conclusion, exfoliated-restacked MoS<sub>2</sub> shows surface-limited intercalation pseudocapacitance behavior which enables ultrafast energy storage with enhanced capacitance of 250 Fg<sup>-1</sup>. Even at the high rate 20C (3 min charge or discharge), a high capacitance of 150 Fg<sup>-1</sup> is still retained. The Li<sup>+</sup> intercalation kinetics is facilitated by exfoliation, which provides a reduced diffusion barrier for Li<sup>+</sup> transport, and the metallic 1T-phase that enhances the electronic conductivity. This study shows the exfoliated-restacked MoS<sub>2</sub> as a promising intercalation pseudocapacitor material for ultrafast energy storage.

## Experimental Section

### Material synthesis and characterization

Commercial molybdenum disulfide (*com*-MoS<sub>2</sub>) powder (Aldrich) was soaked in *n*-butyllithium in hexane (Aldrich) to form Li<sub>x</sub>MoS<sub>2</sub>. The lithiated product was exfoliated in water to form a quasi-stable suspension of single-layered MoS<sub>2</sub>. The suspension was centrifuged, washed with water three times, and dried as restacked sample (*exf*-MoS<sub>2</sub>). The samples were characterized by synchrotron radiation (λ=0.78 Å, Beamline X14A at Brookhaven National Laboratory), X-ray absorption spectroscopy (XAS, Beamline X18 A at Brookhaven National Laboratory), and transmission electron microscopy (TEM, JEOL 2100F).

### Electrochemical characterization

The electrochemical performances of MoS<sub>2</sub> samples were characterized with three-electrode cells using a potentiostat (Biologic

VMP-3). Slurry of the active material (70 wt%), Super-P carbon (20 wt%), and polyvinylidene fluoride (10 wt%) dispersed in *N*-methyl-2-pyrrolidone was spread on a piece of stainless steel (316L) mesh and dried to form the working electrode. Li-ion intercalation experiments were done with 1 M lithium perchlorate (LiClO<sub>4</sub>) in tetrahydrofuran (THF) as the electrolyte and Li foil as the counter and reference electrodes. A solution of 0.25 M [Mg<sub>2</sub>Cl<sub>3</sub>]<sup>+</sup> [AlPh<sub>2</sub>Cl<sub>2</sub>]<sup>-</sup> and 0.5 M lithium chloride (LiCl) in THF served as the electrolyte for a Li-Mg-ion hybrid supercapacitor.

## Acknowledgements

Y.Y. acknowledges funding support from the U.S. Office of Naval Research (No. N00014-13-1-0543).

**Keywords:** energy storage · exfoliated structure · intercalation pseudocapacitance · molybdenum disulfide · supercapacitor

- [1] K. Mizushima, P. C. Jones, P. J. Wiseman, J. B. Goodenough, *Mater. Res. Bull.* **1980**, *15*, 783–789.
- [2] R. Yazami, P. Touzain, *J. Power Sources* **1983**, *9*, 365–371.
- [3] P. He, H. Yu, D. Li, H. Zhou, *J. Mater. Chem.* **2012**, *22*, 3680–3695.
- [4] T. Brezesinski, J. Wang, S. H. Tolbert, B. Dunn, *Nat. Mater.* **2010**, *9*, 146–151.
- [5] V. Augustyn, J. Come, M. A. Lowe, J. W. Kim, P.-L. Taberna, S. H. Tolbert, H. D. Abruña, P. Simon, B. Dunn, *Nat. Mater.* **2013**, *12*, 518–522.
- [6] V. Augustyn, P. Simon, B. Dunn, *Energy Environ. Sci.* **2014**, *7*, 1597–1614.
- [7] M. Acerce, D. Voiry, M. Chhowalla, *Nat. Nanotechnol.* **2015**, *10*, 313–318.
- [8] T. Stephenson, Z. Li, B. Olsen, D. Mitlin, *Energy Environ. Sci.* **2014**, *7*, 209–231.
- [9] F. Wypych, R. Schollhorn, *J. Chem. Soc. Chem. Commun.* **1992**, 1386–1388.
- [10] L. Wang, Z. Xu, W. Wang, X. Bai, *J. Am. Chem. Soc.* **2014**, *136*, 6693–6697.
- [11] J. R. Lince, M. R. Hilton, A. S. Bommannavar, *Thin Solid Films* **1995**, *264*, 120–134.
- [12] Y. Li, Y. Liang, F. C. Robles Hernandez, H. D. Yoo, Q. An, Y. Yao, *Nano Energy* **2015**, *15*, 453–461.
- [13] H. Scher, R. Zallen, *J. Chem. Phys.* **1970**, *53*, 3759–3761.
- [14] L. Jiang, S. Zhang, S. A. Kulinich, X. Song, J. Zhu, X. Wang, H. Zeng, *Mater. Res. Lett.* **2015**, *3*, 177–183.
- [15] L. Jiang, B. Lin, X. Li, X. Song, H. Xia, L. Li, H. Zeng, *ACS Appl. Mater. Interfaces* **2016**, *8*, 2680–2687.
- [16] P. Simon, Y. Gogotsi, B. Dunn, *Science* **2014**, *343*, 1210–1211.
- [17] Y. Liang, H. D. Yoo, Y. Li, J. Shuai, H. A. Calderon, F. C. Robles Hernandez, L. C. Grabow, Y. Yao, *Nano Lett.* **2015**, *15*, 2194–2202.
- [18] P. Kurzweil in *Encyclopedia of Electrochemical Power Sources* (Ed.: J. Garche), Elsevier, Amsterdam, **2009**, pp. 600–606.
- [19] M. Okubo, E. Hosono, J. Kim, M. Enomoto, N. Kojima, T. Kudo, H. Zhou, I. Honma, *J. Am. Chem. Soc.* **2007**, *129*, 7444–7452.
- [20] C.-Y. Lee, A. M. Bond, *Langmuir* **2010**, *26*, 16155–16162.
- [21] B. E. Conway in *Energetics and Elements of the Kinetics of Electrode Processes*, Springer US, Boston, MA, **1999**, pp. 33–65.
- [22] H. D. Yoo, J. H. Jang, B. H. Ka, C. K. Rhee, S. M. Oh, *Langmuir* **2009**, *25*, 11947–11954.
- [23] A. G. Pandolfo, A. F. Hollenkamp, *J. Power Sources* **2006**, *157*, 11–27.
- [24] J. Come, V. Augustyn, J. W. Kim, P. Rozier, P.-L. Taberna, P. Gogotsi, J. W. Long, B. Dunn, P. Simon, *J. Electrochem. Soc.* **2014**, *161*, A718–A725.
- [25] H. D. Yoo, I. Shterenberg, Y. Gofer, R. E. Doe, C. C. Fischer, G. Ceder, D. Aurbach, *J. Electrochem. Soc.* **2014**, *161*, A410–A415.
- [26] G. A. Snook, G. J. Wilson, A. G. Pandolfo, *J. Power Sources* **2009**, *186*, 216–223.

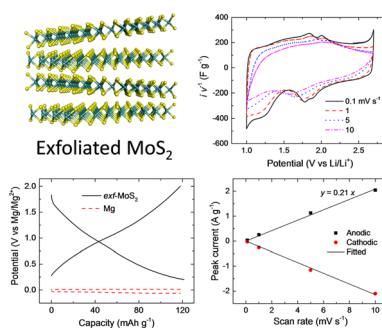
Manuscript received: March 23, 2016

Accepted Article published: April 8, 2016

Final Article published: ■ ■ ■ ■, 0000

## COMMUNICATION

**In the fast lane:** Exfoliated molybdenum disulfide shows  $\text{Li}^+$  intercalation pseudocapacitance with a high capacitance of  $250 \text{ F g}^{-1}$  and a high rate capability that is suitable for ultrafast energy storage.



### Layered Materials

Hyun Deog Yoo, Yifei Li, Yanliang Liang,  
Yucheng Lan, Feng Wang, Yan Yao\*



**Intercalation Pseudocapacitance of  
Exfoliated Molybdenum Disulfide for  
Ultrafast Energy Storage**

